JOURNAL OF SOLID STATE CHEMISTRY 106, 27–34 (1993)

Theory of Point Defects and Vacancy Motion in Corundum Crystals

P. W. M. JACOBS* AND E. A. KOTOMIN†

*Department of Chemistry, The University of Western Ontario, London, Ontario, Canada N6A 5B7; †Institute for Solid State Physics, The University of Latvia, 19 Rainis Blvd., Riga, LV 1098 Latvia

Received December 4, 1992; accepted December 23, 1992

IN HONOR OF SIR JOHN MEURIG THOMAS ON HIS 60TH BIRTHDAY

The energies of formation of Schottky and Frenkel defects in corundum (α-Al_2O_3) have been calculated and also the activation energies for cation and anion vacancy hopping using the method of atom–atom potentials as formulated in the Mott–Littleton strategy and implemented in the CASCADE computer code. Special attention has been paid to the ability of the two-body potentials used to describe the crystal structure and properties and the need to allow for the energy change associated with the relaxation of basis strains. Several mechanisms of oxygen vacancy hopping were also simulated by means of the quantum chemical INDO method which takes into account the covalent contribution of chemical bonding in corundum. These calculations show insignificant increase in the effective charge of the hopping O atom in its saddle point, which justifies the use of atom–atom potentials in this context. The INDO activation energies for vacancy hops reveal the same trend as obtained in CASCADE calculations: where they disagree indicates a failure to optimize ionic displacements completely in the INDO calculation. In agreement with CASCADE calculations these migration energies are much lower when the hopping ion is allowed to deviate from a straight path (typically by 0.3–0.4 Å). Both kinds of calculations predict the activation energy for vacancy hopping between basic structural O triangles to be the factor limiting oxygen migration.

1. Introduction

Corundum (α-Al_2O_3) crystal is of technological importance as a ceramic material (*1*, *2*), as a substrate for thin film growth, in single-crystal IR optical fibers (*3*), as a fusion material, in catalysis, in radiation dosimetry (*4*) and in solid-state lasers (*5*). Despite all these actual or potential applications there have been only two previously published investigations of its defect properties using pair potentials, by Dienes *et al.* (*6*) and by Catlow *et al.* (*7*) (see also Mackrodt (*8*). Both of these investigations used relatively small sizes for the inner explicitly relaxed region immediately surrounding the defect: nor was the importance of the contribution of the strain energy associated with the relaxation of basis strains during minimization of defect energy assessed; and nor was the possibility of nonlinear paths for defect migration investigated. The last two factors will be shown to be of considerable importance in α-Al_2O_3. In addition to our calculations based on pair potentials we have performed quantum chemical calculations for three of the anion vacancy jumps. These confirm the nonlinear paths found from pair-potentials and justify the use of the latter technique by showing that negligible redistribution of ionic charge occurs during the passage of an ion from its initial position to the saddle point configuration.

2. Theoretical Methods

2.1 Cascade Code

Modern computers and programming techniques have made possible tremendous

0022-4596/93 $5.00

advances in computational chemistry in the past twenty years, not least in the calculation of defect energies (*9, 10*) and entropies (*10, 11*) for ionic crystals. It is more than 50 years since the classic paper by Mott and Littleton (*12*) first enunciated the idea of dividing the imperfect crystal into two regions, an inner region I containing the defect D and the ions immediately surrounding D, and region II which is the rest of the crystal. In region I the displacement of the ions are calculated explicitly using potentials that define the short-range (SR) interactions but in region II (see later for a more detailed description) ionic displacements are calculated in a continuum approximation. Long-range (LR) Coulomb interactions are accounted by the usual Ewald procedure. At first, region I was necessarily limited to something like the nearest neighbour (nn) and next nn (2nn) ions to D, but now, region I would generally contain approximately 100–200 ions, depending on crystal and defect symmetry and the complexity of the defect D, which might be some cluster of ions and point defects occupying several unit cells. Some algebraic manipulations (*10*) and the use of the harmonic approximation and equilibrium condition, permit one to express the total energy of the defective crystal in terms of interactions between the (displaced) ions within region I and between the defect and (displaced) ions of region II. An important development (*13*) was the division of region II into an inner part IIa that immediately surrounds I, and an outer part IIb, which is the rest of the crystal. The important property of IIa is that it is sufficiently thick so that SR interactions between I and IIb may be neglected. Then interactions within I and IIa are calculated explicitly from SR pair-potentials and Coulomb's law, while LR interactions between I and IIb are calculated by means of the Ewald procedure. (Actually, one calculates the Coulomb interactions for the whole crystal by Ewald's method and then subtracts off the already explicitly evaluated part: for further details see Refs. (*10, 14*).) The original CASCADE program was limited to two-body SR interactions but subsequent developments (*15, 16*) include the possibility of two kinds of three-body interactions. The energy of the imperfect crystal, E, at equilibrium is evaluated by finding the minimum of E with respect to the positions of the explicitly relaxed ions of region I.

2.2 The Semiempirical INDO Method

Since corundum crystals are partly covalent, which has been confirmed both experimentally (*17, 18*) and theoretically (*19, 20*), we also performed quantum chemical simulations of different mechanisms of vacancy migration in order to estimate the role of charge redistribution during atomic hopping and thus to check the applicability of pair-potential techniques and the purely ionic model used here for corundum.

The method used was the semiempirical self-consistent intermediate neglect of differential overlap (INDO method) (*21, 22*) combined with the embedded molecular cluster model (*23*).

The basis set includes $3s$, $3p$ atomic orbitals (AO) on Al and $2s$, $2p$ AOs on O. These INDO parameters were optimized via calculating the properties of a series of di- and triatomic molecules containing Al and O atoms and the electronic structure of the perfect bulk corundum crystal (*24*). The effective charges on the ions calculated by means of the periodic large-unit-cell model (*25–27*) are $-1.5\ e$ on O and $2.34\ e$ on Al atoms (e is the proton charge) which are in good agreement with *ab initio* calculations (*19*). The optimized lattice parameter is only 5% less than the experimental value while the calculated bulk modulus $B = 358$ GPa exceeds the experimental value by 15%.

In defect calculations we used several different stoichiometric clusters, $[Al_4O_6]$, $[Al_8O_{12}]$, and $[Al_{14}O_{21}]$, embedded into the crystalline field of the rest of the crystal. Before inserting an O vacancy (or hole) at the center of the cluster, boundary atoms were allowed to relax until the total energy was a minimum, thus taking into account the

effect of the bond breaking between these atoms entering the quantum cluster and their neighbors, which are simulated by non-point charges.

3. Results and Discussion

3.1 Pair-Potentials and Basis Strains

Three kinds of crystal potentials were considered for corundum. The first of these was that derived previously by Catlow, James and co-workers (*7*). It gives a reasonable fit to crystal properties, the cohesive energy, elastic constants and permittivity, and also the lattice constants (that is, at the experimental lattice constants the potential gives reasonably low bulk lattice strains), but it has the disadvantage of providing quite large basis strains. This means that the equilibrium (minimum energy) structure predicted by the potential does not quite coincide with that determined experimentally (*28*). The Catlow and James potential for corundum is based on an O^-–O^- potential (*29*) which had been determined by Hartree–Fock (HF) calculations for O_2^{2-} surrounded by four positive charges in a tetrahedral configuration. The remaining Al^{3+}–O^{2-} Buckingham parameters and the shell-model shell-charges and core-shell force-constants were determined by fitting crystal data. O_2^{2-} is not a stable species in free space and nor is O^{2-}, so Jacobs and Vernon (*30*) determined their O^{2-}–O^{2-} potential by using the conserved charge-density approximation and ionic charge densities from HF calculations on an O^{2-} ion in a simulated crystal field. They also allowed for damping of the dispersion interaction due to charge overlap. This potential was quite successful in reproducing crystal properties of MgO and Li_2O (*31*) and when combined with the Al^{3+}–O^{2-} potential from Catlow *et al.* (*7*) it also gave (after some very minor adjustments) a reasonably good representation of the properties of corundum, with somewhat smaller basis strains. Both these potentials use the full formal charges of $+3e$ for Al and $-2e$ for O. It is possible, in principle, to derive a corundum potential (*31*) using the reduced ionic charges indicated by quantum chemistry (*24*) and this potential does indeed lead to very small bulk lattice strains. However, because ionic charges that are less than the formal valence charges of $+3$ for Al and -2 for O, the perfect-crystal cohesive energy is indeterminate from a purely pair-potential calculation, though it could be calculated quantum-chemically. Because our interests at this stage lay in defect calculations from pair-potentials, we did not pursue further the search for potentials with other than formal ionic charges. This, perhaps, may be considered a limitation of the pair-potential approach to defect calculations on partly covalent materials: nevertheless a fully ionic representation works quite well for corundum as well as other partly covalent materials. Corundum has a complicated crystal structure and probably requires many-body forces for an adequate representation of its bonding, so that it is a far from ideal test case. Because the Jacobs and Vernon oxygen potential led to slightly higher bulk lattice strains than the Catlow and James corundum potential, we finally decided to use only the latter. However, either the basis strains must be relaxed first, and the potential refitted, or the strain energy must be determined in a separate calculation and subtracted off from the defect energy, which otherwise includes the strain energy if the structure is not fully relaxed first. The energy to form Schottky and Frenkel defects, after correction for crystal relaxation shows very little dependence on the size of region I (*28*) so that further calculations may be done with a region I that contains ~150 ions.

3.2 Defect Formation and Migration Energies

The calculated defect energies from the CASCADE program for the formation of

TABLE I

CALCULATED COHESIVE ENERGY (PER Al_2O_3) AND DEFECT FORMATION ENERGIES (PER DEFECT) FOR CORUNDUM, IN eV, USING THE CATLOW AND JAMES POTENTIAL (7) REFITTED AFTER REMOVAL OF BASIS STRAINS

	Energy/eV
Cohesive energy	−160.24
Cation vacancy	55.41
Anion vacancy	24.65
Cation interstitial	−42.54
Anion interstitial	−14.39
Schottky defect	4.91
Cation Frenkel defect	6.43
Anion Frenkel defect	5.13

Note. Region I contained $N \geq 150$ ions.

vacancies and interstitials in corundum are given in Table I, together with the energies to form a Schottky defect and a Frenkel defect on either the cation or anion sublattice. (These energies are given in eV/defect so that the energy to form a Schottky quintet, for example, is 5×4.91 eV = 24.55 eV.) The defect energies indicate a very slight preference for Schottky defects over anion Frenkel defects, but the energy difference is so slight that clearly both Schottky and anion Frenkel defects should be taken into account in any analysis of ionic transport in pure corundum. However, the high value of the formation of cation Frenkel defects makes it unlikely that there are a substantial number of cation interstitials. These calculated values in Table I refer to a region I size that contained $N \geq 150$ ions (the precise number depending on the type of defect). With proper allowance for basis strains the defect energies are sensibly independent of region I size, making an extrapolation to $N = \infty$ unnecessary. Accordingly, a region I size of $N \geq 150$ was used in all further calculations.

The activation energy for anion and cation motion along various paths was investigated by calculating the saddle-point energy. For some of the jumps, a curved path between the initial and final sites was investigated. If the saddle point lies on a plane of symmetry normal to the linear path joining initial and final sites, then it may be located automatically by the CASCADE minimization procedure. But (as is more usually the case) the moving ion is not prevented by symmetry from returning to its initial state or proceeding to its final state, the calculation will fail to locate the saddle point. In this situation the moving ion must be fixed at a number of arbitrarily chosen positions and the potential energy surface probed to locate the minimum. The anion and cation paths investigated are shown in Fig. 1. For $a1$, $a2$, and $a4$ the saddle-point minima lie at points displaced by Δ from midpoints of linear paths, along lines normal to the linear paths. For $a3$ and $a5$ linear paths were assumed. For cation jumps $c1$–$c4$ linear paths are expected. A curved path was investigated for $c5$ but a linear path was confirmed. Figure 2 shows the energy change from a starting configuration, ΔE, in the neighborhood of the saddle point, as a function of the displacement Δ in a plane normal to the path of the jump, for $a1$, $a2$, and $a4$ jumps. For $c5$, the defect energy E is plotted against the z coordinate; $z = 0.333$ corresponds to $\Delta = 0$. So for $c5$ the linear path requires the least energy. Activation energies and path displacements Δ are given in Table II.

3.3 INDO calculations

When an O vacancy is inserted into the corundum lattice, INDO calculations show that the two O atoms entering the same basic triangle are displaced toward it by 6% of the O–O distance (2.39 Å) which results in an energy gain of 0.61 eV, in good agreement with CASCADE calculations. Then we simulated three kinds of O vacancy hops, enumerated 1, 2, 3 in Fig. 1 and discussed above in Section 3.2—inside small basic O triangles, in big triangles, and between small triangles belonging to the different oxygen planes. The calculated energies are also given in Table II. The INDO hopping energies for $a2$ agrees very well with the

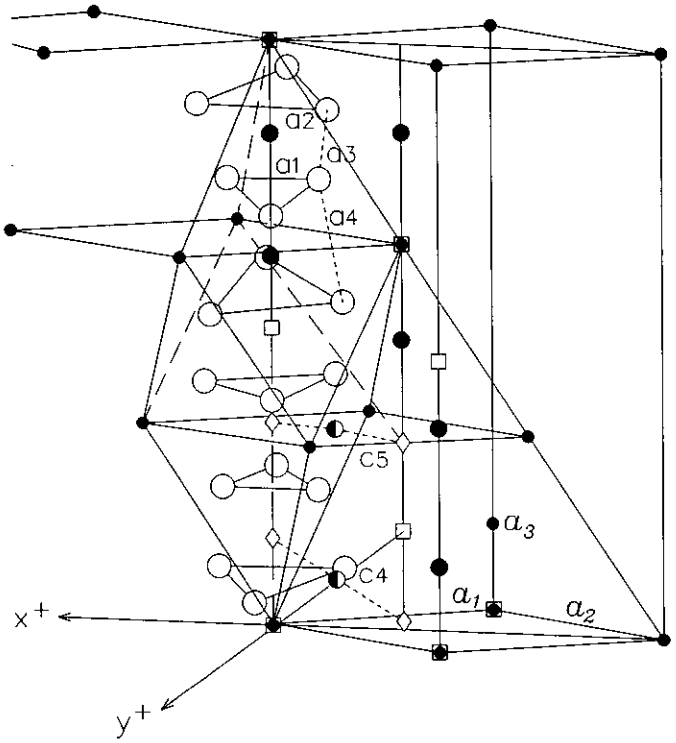

FIG. 1. Portion of the crystal structure of corundum showing the definition the of anion jumps $a1, \ldots, a4$ and cation jumps, $c4$, $c5$.

CASCADE value. For $a1$, the INDO value is larger by 0.19 eV and for $a3$ it is much larger than the CASCADE result, almost certainly because we failed to relax the lattice properly in this instance. Two principal conclusions may be drawn here, in complete agreement with the CASCADE calculations: (i) the activation energy for a vacancy hop in a small triangle is much lower than in a big triangle and/or between small triangles; (ii) the deviation of the hopping O atom from a straight line can greatly reduce the activation energy (Fig. 2). Since O vacancy migration occurs by combining hops 1 and 3 both methods used predict the activation energy for hops 3 between small triangles to be the limiting factor; our estimate of 1.85 eV is in good agreement with the revised experimental value of Oishi of 1.86 eV (*32*). The deviations of the hopping atom in its saddle point from the straight line connecting the two O sites found by the two different techniques used here, were reassuringly similar (see Table II); this, however, has a greater effect on the INDO activation energies. Previous studies (*33*) of ion migration in corundum assumed linear paths and our calculations show that results obtained with linear paths will be much too high. One of the main INDO results is that the effective charge of the hopping O atom in the saddle point does not change very much, compared with that of an O^{2-} ion on a regular lattice site (cf., $-1.63\ e$ and $-1.53\ e$ respectively) which justifies the use of atom–atom potentials for saddle point calculations.

4. Conclusions

In this paper we have shown that realistic two-body potentials may be derived for co-

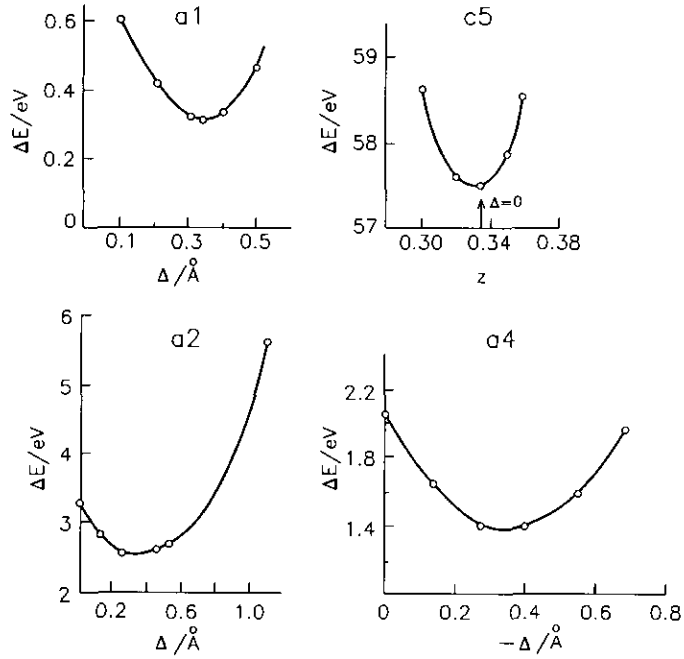

FIG. 2. For $a1$, $a2$, and $a4$, figures show the energy change ΔE (in eV) from initial configuration (with all ions on lattice sites) as a function of Δ the displacement (in Å) at the saddle point in a direction normal to the linear path between initial and final states. In $c5$ the plot of defect energy E against the z coordinate (cf., Fig. 1) shows that the path of the jump is a linear one since $z = 0.333$ corresponds to the saddle point on the linear path.

rundum which gave a fairly good description (*28*) of perfect crystal static lattice properties and sensible defect energies. Comparison with experimental transport properties is not straightforward because of doubts about crystal purity and the strong association between divalent impurity ions and oxygen vacancies. Further work will include calculations of the lattice dynamics and the investigation of the possible importance of three-body forces (*16, 34*) in α-Al_2O_3. No two-body potential derived so far for corundum that fits the crystal properties, including the cohesive energy, is free of basis

TABLE II

ACTIVATION ENERGIES ΔE (IN eV) FOR ANION AND FOR CATION MOTION IN CORUNDUM

CASCADE			INDO		CASCADE	
Path	Δ/Å	ΔE/eV	Δ/Å	ΔE/eV	Path	ΔE/eV
$a1$	0.34	0.34	0.42	0.49	$c1$	3.69
$a2$	0.33	2.50	0.32	2.56	$c2$	0.56
$a3$	—	1.85	—	3.50	$c3$	2.29
$a4$	0.34	1.37	—	—	$c4$	3.76
$a5$	—	5.10	—	—	$c5$	2.06

Note. For curved paths the displacement Δ (in Å) of the saddle point from a linear path in a direction normal to a linear path is given.

strains (cf., section 3.1). Relaxation of basis strains gives a large contribution to the calculated defect energy (*28*) which must be accounted for unless the crystal structure is relaxed first. This affects particularly the components of the static permittivity tensor which must therefore be refitted. Such potentials display only a very small dependence of defect energy on region I size so that extrapolations to an infinite region I ($N \rightarrow \infty$) are unnecessary in this case, provided a reasonably large region I is used. The region I size of $N \geq 150$ used in this work is certainly adequate, though it is large enough to make heavy demands on cpu time, when a large number of defects and paths have to be simulated.

We have shown that the deviation of the migrating atom from a straight line path can greatly reduce the hopping activation energy. The results of calculations made using atom–atom potentials agree quite well with those of the quantum chemical approach which gives more confidence to our conclusions. Negligible charge redistribution observed in the quantum-chemical calculations justifies the use of atom–atom potentials in these computer simulations of ionic migration. Finally, we should mention that we have also investigated the possibility of valence-band holes in corundum becoming self-trapped (*24*, *35*) or trapped at cation vacancies or Mg^{2+} substitutionals (*36*) and also the motion of self-trapped holes (*37*).

Acknowledgment

EAK thanks the Centre for Chemical Physics for the award of a Senior Visiting Fellowship and for the warm hospitality accorded him by Centre members. PWMJ acknowledges continuing support from the National Sciences and Engineering Research Council of Canada in the form of a Research Grant and an International Collaborative grant, and The University of Western Ontario for financial support from the Special Competition for NSERC funds. It is a pleasure to take this opportunity to acknowledge the tremendous leadership role of Sir John Meurig Thomas in the field of Solid State Chemistry, and the support that so many who practice its art and science have received from him, both personally and collectively.

References

1. W. D. KINGERY (Ed.), "Structure and Properties of MgO and Al_2O_3 Ceramics." *Adv. Ceram.* **10** (1983).
2. R. H. FRENCH, *J. Am. Ceram. Soc.* **73,** 477 (1990).
3. G. MERZBERG AND J. W. HARRINGTON, "Infrared Fibre Optics III," Proceedings of SPIE, No. 1591.
4. J. A. VALBIS AND N. ITOH, *Radiat. Eff. Def. Solids* **116,** 171 (1991).
5. E. F. MARTYNOVICH, V. I. BARYSHNIKOV, AND V. A. GRIGOROV, *Opt. Commun.* **53,** 257 (1985).
6. G. J. DIENES, D. O. WELCH, C. R. FISCHER, R. D. HATCHER, O. LAZARETH, AND M. SAMBERG, *Phys. Rev. B* **11,** 3060 (1975).
7. C. R. A. CATLOW, R. JAMES, W. C. MACKRODT AND R. F. STEWART, *Phys. Rev. B* **25,** 1006 (1982).
8. W. C. MACKRODT, *in* "Structure and Properties of MgO and Al_2O_3 Ceramics" (W. D. Kingery, Ed.) *Adv. Ceram.* **10,** 62 (1983).
9. P. W. M. JACOBS, *J. Chem. Soc. Faraday Trans. 2* **85,** 415 (1989).
10. P. W. M. JACOBS, *in* "Diffusion in Materials" (A. L. Laskar, J. L. Bocquet, G. Brébec, and C. Monty, Eds.) p. 203, Kluwer Dordrecht (1990).
11. P. W. M. JACOBS, *Chem. Soc. Faraday Trans. 2* **86,** 1197 (1990).
12. N. F. MOTT AND M. J. LITTLETON, *Trans. Faraday Soc.* **34,** 485 (1938).
13. M. J. NORGETT, AERE Harwell Report R-7650, HM Stationery Office, London (1974).
14. W. C. MACKRODT, *J. Comp. Phys.* **44,** 206 (1981).
15. M. LESLIE, *Physica B* **131,** 145 (1985).
16. R. C. BAETZOLD, C. R. A. CATLOW, J. CORISH, F. M. HEALY, P. W. M. JACOBS, M. LESLIE, AND Y. T. TAN, *J. Phys. Chem. Solids* **50,** 791 (1989).
17. H. BIALAS AND H. J. STOLZ, *Z. Phys. B* **21,** 319 (1975).
18. J. LEWIS, D. SCHWATZENBACH, AND H. D. FLACK, *Acta Crystallogr Sect. A* **38,** 733 (1982).
19. M. CAUSA, R. DOVESI, C. ROETTI, E. KOTOMIN, AND V. SAUNDERS, *Chem. Phys. Lett.* **140,** 120 (1987).
20. L. SALASCO, R. DOVESI, R. ORLANDO, M. CAUSA, AND V. SAUNDERS, *Mol. Phys.* **72,** 267.
21. J. A. POPLE AND D. L. BEVERIDGE, "Approximate Molecular Orbital Theory," McGraw-Hill, New York 1970.
22. E. STEFANOVICH, E. SHIDLOVSKAYA, A. SHLUGER, AND M. ZAKHAROV, *Phys. Status Solidi* **160,** 529 (1990).
23. A. SHLUGER, L. KANTOROVICH, AND E. KOTOMIN, *J. Phys. C Solid State Phys.* **19,** 4183 (1986).
24. P. W. M. JACOBS, E. A. KOTOMIN, A. STASHANS,

E. V. STEFANOVICH, AND I. TALE, *J. Phys. Cond. Matter* **4,** 7531 (1992).

25. R. A. EVARESTOV, "Quantum Chemical Methods in Solid State Theory," Leningrad Univ. Press (1982).
26. R. A. EVARESTOV AND V. A. LOUCHIKOV, *Phys. Status Solidi B* **91,** 743 (1977).
27. R. A. EVARESTOV AND V. A. LOUCHIKOV, *Phys. Stat. Solidi B* **93,** 469 (1979).
28. P. W. M. JACOBS AND E. A. KOTOMIN, *Philos. Mag. A*, in press.
29. C. R. A. CATLOW, I. D. FAUX, AND M. J. NORGETT, *J. Phys. C* **9,** 419 (1976).
30. P. W. M. JACOBS AND M. L. VERNON, *J. Chem. Soc. Faraday Trans. 2* **86,** 1233 (1990).
31. J. D. GALE, personal communication.
32. Y. OISHI AND W. D. KINGERY, *J. Chem. Phys.* **33,** 480 (1960); Y. OISHI AND K. ANDO, *Adv. in Ceramics* **10,** 379 (1983).
33. R. JAMES, Ph.D. thesis. Also available as AERE Harwell Report TP 814, HM Stationery Office, London (1979).
34. C. R. A. CATLOW, C. M. FREEMAN, AND R. L. ROYLE, *Physica B* **131,** 1 (1985).
35. P. W. M. JACOBS AND E. A. KOTOMIN, *Phys. Rev. Lett.* **69,** 1411 (1992).
36. P. W. M. JACOBS, E. A. KOTOMIN, A. STASHANS, AND I. TALE, *Mat. Sci. Eng.*, in press.
37. P. W. M. JACOBS, E. A. KOTOMIN, A. STASHANS AND I. A. TALE, *Philos. Mag. B*, **67,** 557 (1993).